DOI: 10.2478/jlecol-2026-0023 Journal of Landscape Ecology (2026), Vol: 19 / No. 3

ASSESSING OF THE SPATIO-TEMPORAL CLIMATE AND AIRBORNE POLLUTION CHANGES AND TRENDS IN UKRAINIAN STEPPE ZONE

MYKOLA KHARYTONOV[1*], PETRO LAKYDA[2], LIUBOV MATUSHEVYCH[2], ARTEM ANDREIEV[3], ANNA KOZLOVA[3] AND SERGEY STANKEVICH[4]

[1]*Center of Nature Agriculture, Dnipro State Agrarian and Economy University, Ukraine, Dnipro,49009, Serhii Yefremov st., 25*
[2]*Department of Forest Mensuration and Forest Management, National University of Life and Environmental Sciences of Ukraine, Ukraine, Kyiv, 03041, Heroyiv Oborony st., 15*
[3]*Department of Geoinformation Technologies in Remote Sensing of the Earth, Scientific Centre for Aerospace Research of the Earth, National Academy of Sciences of Ukraine, Ukraine, Kyiv, 01054, Oles Gonchar st., 55B*
[4]*Department of Geospatial Modelling in Aerospace Research, Scientific Centre for Aerospace Research of the Earth, National Academy of Sciences of Ukraine, Ukraine, Kyiv, 01054, Oles Gonchar st., 55B*
**Corresponding author email: kharytonov.m.m@dsau.dp.ua*

Received: 16th August 2025, **Accepted:** 26th November 2025

ABSTRACT

Land cover changes in arid zones with industrial agglomerations require a comprehensive spatiotemporal assessment of drought and soil airborne pollution. Geospatial maps were obtained for each level of the two time periods -2019-2021 and 2022-2024 based on the distribution and contextual significance of each parameter. An analysis of the identified trends in the climate change indicators (precipitations, evapotranspiration and land surface moister) allows us to speak about a meteorological type of drought complicated with large Kakhovka water reservoir disappearance in June 2023. At the same time, the advance of drought conditions was fixed in the LAI change in canopy density throughout the steppe zone of Ukraine by 2024. It was found that the progression of arid conditions has the character of horizontal zonality in the direction from south to north.

The main differences in the risk of acid rain caused by industrial agglomerations are related to the spatial distribution of nitrogen dioxide in the atmosphere in the northern part of Ukrainian steppe.

Keywords: Steppe zone, spatio-temporal climate changes, land surface temperature and moister, leaf area index, airborne emissions.

INTRODUCTION

Soil moisture is one of the most critical land environmental variables in assessing terrestrial environmental conditions associated with ecological, hydrological, and atmospheric processes (Sellers & Schimel, 1993; Goward *et al.*, 2002). Variations in soil moisture lead to significant changes in the surface energy balance, regional runoff, and vegetation productivity. Land surface temperature (LST) is an important parameter for understanding the surface energy balance and the exchange of heat between the Earth's surface and the atmosphere (Weng *et al*., 2004; Weng, 2009). It is known that drought is expressed in prolonged water scarcity and can last for months and even years (Alahacoon & Edirisinghe, 2022; Jalayer *et al*., 2023). Comparison of VI and LST showed that the values of the three indices mentioned decreased, and LST increased. A spatiotemporal study of vegetation health and drought severity in southern Africa showed that the spatial trend of land surface temperature (LST) and NDDI has increased in recent years in the range from moderate drought to the severe drought threshold (Orimoloye *et al*., 2019). A decrease in SSM leads to an increase in the daily range of LST, and the maximum LST occurs later under wet conditions because dry soils respond more quickly to temperature variations than wet soils (Sun & Pinker, 2004).

Leaf Area Index (LAI) is defined as the one-sided green leaf area per unit ground area for broadleaf canopies or the projected needleleaf area for coniferous canopies (Tian, 2024). The assessment of leaf area index is linked to vegetation cover, soil temperature and moisture change processes and climate modelling (Avdan & Jovanovska 2016). Understanding changes in land cover and land surface temperature (LST) is important for assessing ecological and climate processes and land management (Ahmed *et al*., 2024). The interaction between thermal and vegetation dynamics, in connection with different land cover types, results in changes in spectral radiance and texture in LST (Weng *et al.,* 2004). These differences are responsible for the spatial patterns of urban heat island movement. The urban heat island effect has been established not only for large agglomerations (Gallo & Owen, 1998) but also in cities with a population of less than 10,000 people (Karl *et al*., 1988). Natural vegetation is replaced by surfaces such as asphalt, stone, metal and concrete. As a result, the level of evapotranspiration of such surfaces is sharply reduced. It leads to an increase in heat flux. Differences in heat fluxes are due to different relative rates of surface cooling between urban and rural areas (Voogt, 2002; Weng & Schubring, 2004). In this regard, the role of vegetation in reducing the amount of heat stored in the soil and surface structures due to transpiration, in contrast to relatively unvegetated urban areas, has been called a significant factor in reducing the formation of heat islands (Carlson *et al*., 1981; Goward, 1981). Most of the changes caused by urbanization were observed as the TVX space transitioned from low temperatures and dense vegetation conditions to high temperatures and sparse vegetation conditions (Amiri *et al*., 2009). Normalized Differrence Vegetation Index (NDVI), urban vegetation abundance (UVA) and urban forest abundance (UFA) were found to be negatively correlated with LST (Huang *et al.*, 2009). Thus, urban vegetation and urban forest are able to reduce LST. Sustainable redevelopment of urban brownfields requires accurate information on the environmental impact of installing different types of vegetation （Smetana & Crittenden, 2014）. The professional selection and use of native plants can provide alternatives for redeveloping these areas into green spaces. Ecological corridors are also crucial for achieving ecoclimatic regulation goals, such as biodiversity and carbon sequestration enhancement (Wu & Convertino, 2025). Meanwhile, air quality issues caused by acid rains (AR) have become increasingly serious in the cities of industrial regions in recent decades (Payus *et al.,* 2020). AR can be defined as a combination of dry and wet deposition from the atmosphere having higher than normal concentrations of nitric (HNO_3), sulfuric acids (H_2SO_4), and acidifying compounds that lead to a decrease in the pH of rainwater < 5.6 (Prakash *et al*, 2023). AR human-induced sources include the burning of coal, natural gas, and oil in thermal power plants. AR spread and loss result in leaf loss, growth inhibition, premature defoliation, premature senescence, necrotic spots, and other visible plant symptoms (Du *et al*. 2017; Liu *et al*. 2018). Urban and suburban forests can mitigate nitrogen gas pollution by absorbing NO_2 through leaf gas exchange (Gong *et al*., 2022). The average annual NO_2 uptake by urban forests can account for 0.14–2.60 % of annual total atmospheric NO_2 and potentially reduce NO_2 concentrations by an average of 0.10–0.34 g/m.

The main objective of this case study was to study the spatio-temporal climate and airborne pollution changes and trends that occurred during two time periods -2019-2021 and 2022-2024 at the territory of the steppe zone of Ukraine.

MATERIAL AND METHODS

The steppe zone occupies the southern part of Ukraine. It is spread from southwest to northeast up to 1100 km, and from north to south up to 500 km. Its total area is about 25 million hectares, which makes up 40% of the whole territory of the country (Fileccia *et al*., 2014). The main component of the formation of the water regime of the steppe zone of Ukraine is associated with atmospheric precipitation, since groundwater lies at a depth of more than 10 m. Russian forces have destroyed one-third of Ukraine's freshwater storage since February 2022 to 2024 (Hapich *et al.*, 2024; Hapich & Onopriienko, 2024). Potable, industrial and irrigation water supplies have been cut across the south and east of Ukraine. In conditions of insufficient soil moisture, the type of water regime in the northern steppe zone can be characterized as non-washable and, sometimes (once every 5-10 years), washable or sporadically washable. The change in soil cover from ordinary to southern black soils occurs with a decrease in precipitation from 544 mm (north) to 458 mm (south) and an increase in temperature from 8.1 to 9.4 °C. MAPFU official statistics estimate that about 500 million tonnes of soil are lost annually from 32.5 million ha of arable lands in Ukraine (Bulygin, 2006). It means that an average of 15 tonnes per year is eroded from arable land. The following indicators: 1) surface soil moisture (SSM), 2) land surface temperature (LST), 3) leaf area index (LAI), 4) atmospheric NO_2 and SO_2 concentrations were selected to estimate the changes in environmental conditions within the study area. The geospatial maps for each indicator were obtained for two time periods, namely 1)2019 – 2021, 2) 2022 – 2024 and 3) the difference between these periods using the remotely sensed datasets. Each averaged map was divided into five levels: very low, low, medium, high, and very high. These levels were used to standardize visual interpretation across all indicators. However, the specific value ranges for each level were individually determined for each indicator, based on their distribution and contextual meaning.

The data for evapotranspiration analysis were sourced from the MODIS MOD16A2 product (Running *et al.,* 2017). This product provides an 8-day composite with 500 m spatial resolution. Units are given in kg/m^2/8day

Air temperature and precipitation were obtained from the ERA5-Land dataset (Muñoz-Sabater, 2019) with a spatial resolution of 11132 m. Air temperature is given as a daily mean in Kelvin, while precipitation is given as a daily sum in meters. Further, air temperature and precipitation were converted to degrees Celsius (°C) and millimetres (mm), respectively. For each year from 2019 to 2024, evapotranspiration and air temperature data were averaged annually over the vegetation period (April-September), while precipitation was calculated as the total sum over the vegetation period.

Surface soil moisture (SSM) data derived from the National Aeronautics and Space Administration (NASA) Soil Moisture Active Passive (SMAP) dataset (Chan *et al.,* 2017). SMAP provides data with 9 km spatial resolution and daily temporal resolution. It indicates the volumetric water content of the soil's upper layer, expressed as a fraction between 0 and 1. The data obtained was averaged for the vegetation period. LST was obtained from the

MODIS MOD11A1.061 product (Wan *et al.,* 2015) with 1 km spatial resolution and daily temporal resolution. The units of measurement are degrees Celsius. This data was averaged only for the vegetation period. The canopy density was evaluated by Leaf Area Index (LAI), which is derived from the MODIS MCD15A3H.061 product (Myneni *et al.,* 2015) with 0.5 km spatial resolution and 4-day temporal resolution. LAI ranges from 0 to 1, where higher values indicate denser green vegetation. Unlike SO_2 and NO_2 concentration, this data was averaged only for the vegetation period (April – September) during the abovementioned years. Atmospheric NO_2 and SO_2 concentrations were assessed by the Sentinel-5p dataset (Veefkind *et al.,* 2012) with 1,1132 km spatial resolution and 2-day temporal resolution (i.e. the data available every 2 days). Thus, we averaged all available data for the two mentioned periods. This dataset provides values presented in mol/m^2. The corresponding map color, value range, area, and share relative to the total area for each of the five levels. The differences between the two periods were marked with green color.

RESULTS

The data on spatially averaged annual seasonal precipitation and evapotransiration in two steppe subzones are shown at the Figs. 1 and 2.

Fig. 1: Annual averaged seasonal precipitation, mm

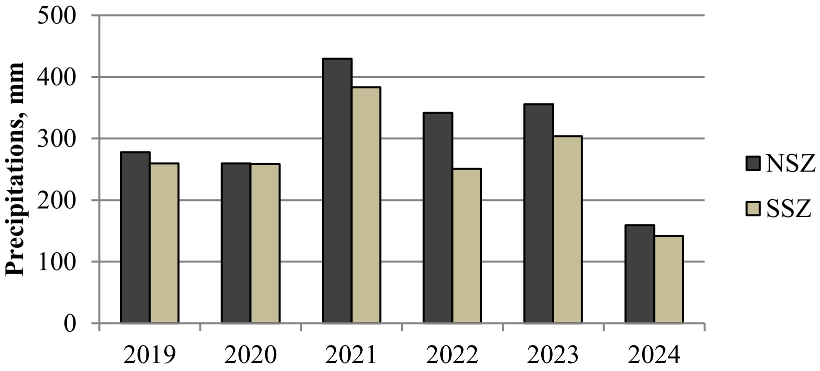

Fig. 2: Annual averaged seasonal evapotranspiration, kg/m^2/8day

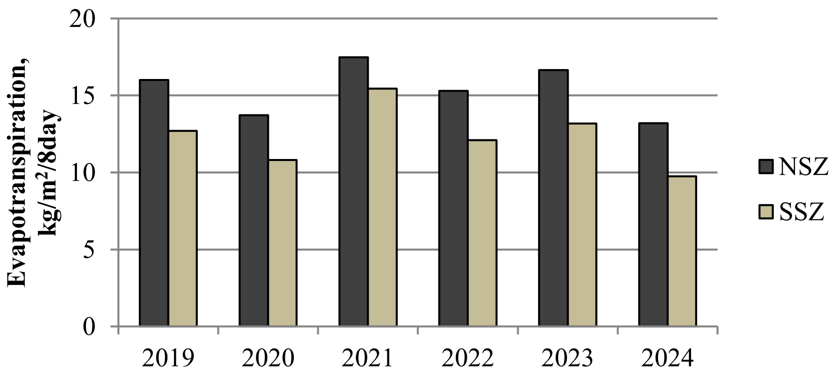

A comparative analysis of the dynamics of changes in average daily seasonal precipitation revealed a significant decrease in 2024. A similar trend was also noted in the decrease in vegetation cover evapotranspiration.

The maps of the spatial distribution of soil moisture across the steppe zone of Ukraine for the two periods being compared are shown in Fig. 3.

Fig. 3: The maps of the surface soil moisture spatial distribution in the steppe zone of Ukraine

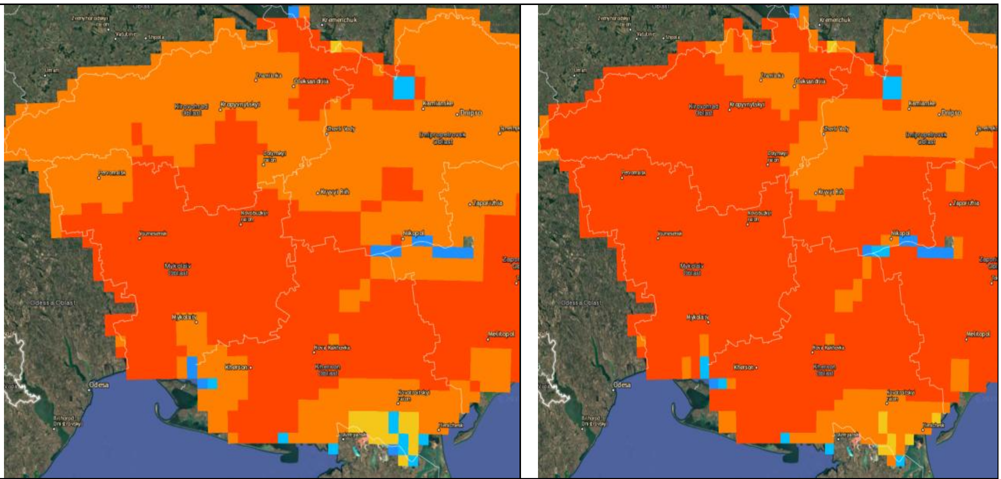

2019-2021	2022-2024

The overall decrease in the spatial distribution of surface soil moisture (SSM) was observed over an area of 34,344 m^2 in four categories in the range of 0.15-0.35 to very low, amounting to 24.23 % (Table 1).

Table 1: Spatial distribution of time-series parameters of SSM

Color	Range	Level	Area (km^2)		Share (%)	
			2019-2021	2022-2024	2019-2021	2022-2024
	0-0.15	Very Low	72090	106434	50.86	75.09
	0.15-0.2	Low	61641	30132	43.49	21.26
	0.2-0.25	Medium	3078	2106	2.17	1.49
	0.25-0.35	High	1944	1053	1.37	0.74
	>0.35	Very High	2997	2025	2.11	1.43
		Decrease	125064		88.23	
		No Change	243		0.17	
		Increase	16443		11.6	

A trend toward meteorological drought by the end of the second period was recorded over an area of 125,064 km^2, accounting for 88 %. The remaining changes occurred with the retreat of water along the Dnipro River bed after the destruction of the Kakhovka Dam by military action in June of 2023 (Fig. 4).

Fig. 4: Differences in the SSM spatial distribution during two periods

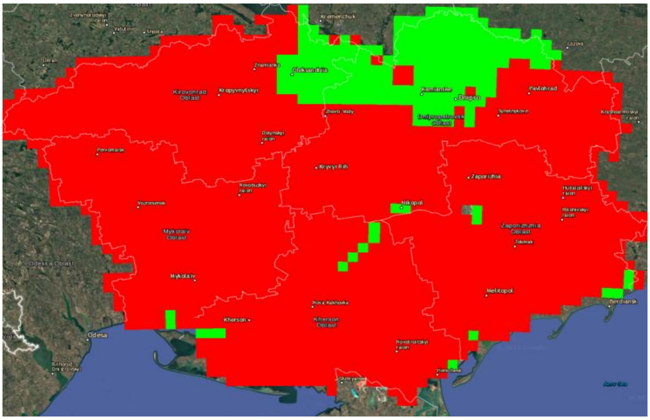

The maps of the spatial distribution of LST across the steppe zone of Ukraine for the two periods being compared are shown in Fig. 5.

Fig. 5: The maps of the spatial distribution of LST across the steppe zone of Ukraine for two compared periods

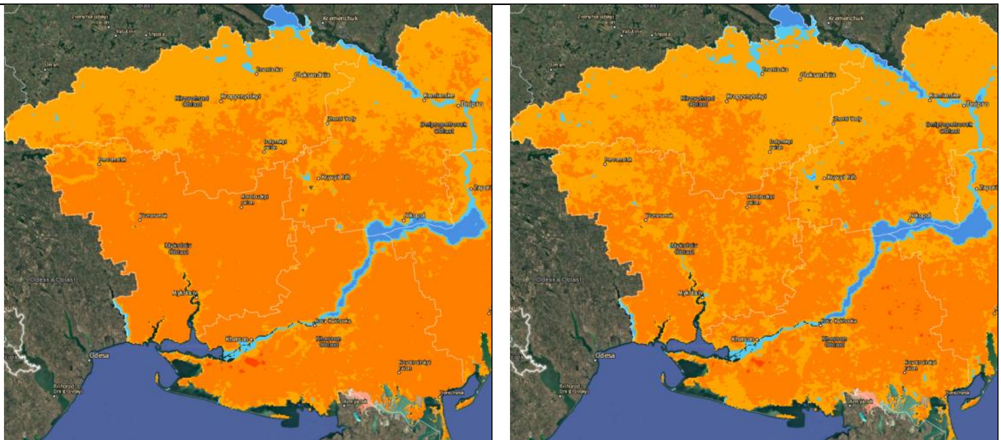

2019-2021	2022-2024

An excess of LST>35^{0}C was recorded in the northern part of the Kherson region over an area of 37 km^2 (Table 2). The share of redistribution of land temperature from high to medium level amounted up to15 % by the end of the second period.

Table 2: Spatial distribution of time-series parameters of LST

Color	Range	Level	Area (km^2)		Share (%)	
			2019-2021	2022-2024	2019-2021	2022-2024
	15-20	Very Low	2006	2431	1.51	1.83
	20-25	Low	2435	3323	1.83	2.5
	25-30	Medium	40193	60940	30.19	45.78
	30-35	High	88356	66257	66.37	49.77
	>35	Very High	139	176	0.1	0.13
		Differences in spatial distribution of LST				
		Decrease	104325		78.37	
		No Change	0		0	
		Increase	28802		21.63	

Differences in the LST spatial distribution for two periods are shown in the Fig. 6.

Fig. 6: The map of the differences in the LST spatial distribution during two periods

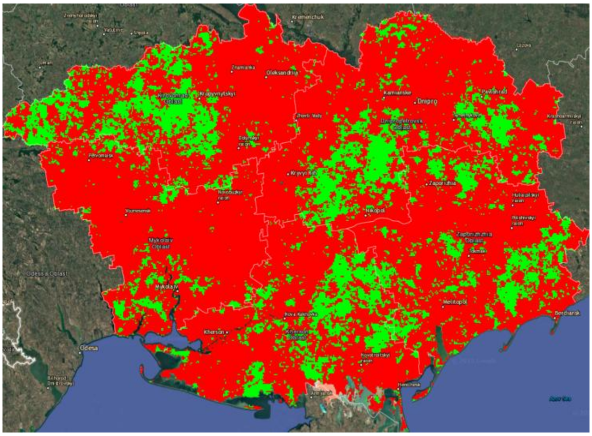

A visual assessment of Fig. 6 allows the identification of areas of spatial changes in land surface temperature, which increased for two years compared to three years, in the green spots at the northwest, centre, south, and western parts of the steppe zone. The share of the LST increasing was 21.6 % on the area 28,8 km^2. A comparative analysis of the dynamics of changes in average daily air temperature indicates the development of drought conditions in both subzones in 2024 (Fig. 7).

Fig. 7: Annual spatial averaged seasonal daily air temperature, ^{0}C

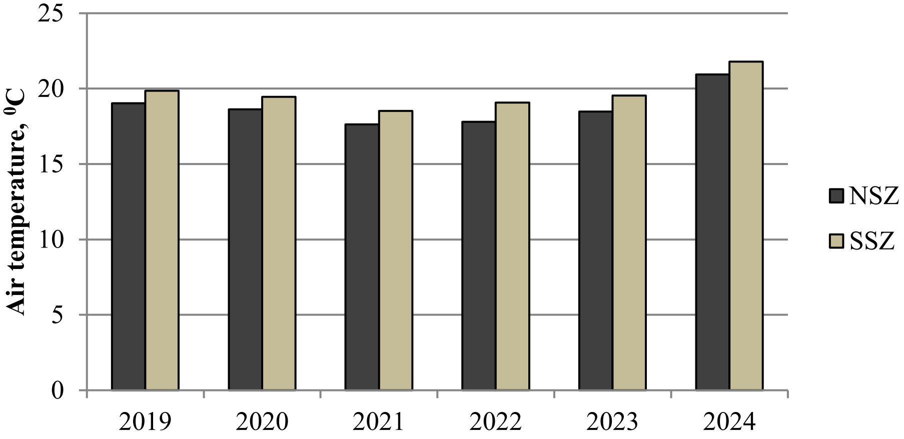

This was a recorded trend of increasing in daily air temperature over the last period from 2022 to 2024. The maps of the spatial distribution of the leaf area index across the steppe zone of Ukraine for the two compared periods are shown in Fig. 8.

Fig. 8: The maps of the leaf area index spatial distribution in the steppe zone of Ukraine

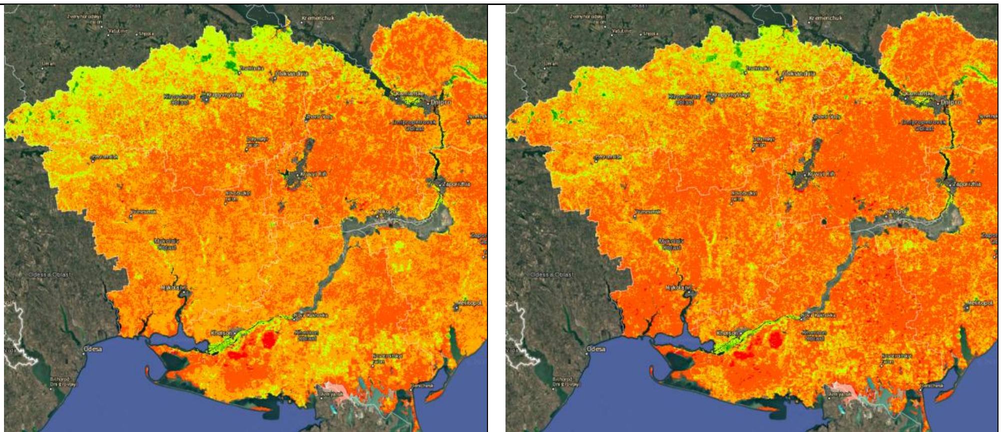

2019-2021	**2022-2024**

It was found that the progression of arid conditions exhibits a character of horizontal zonality from south to north. A similar trend was noted in the LAI change in the canopy density throughout the territory of the northern part of the steppe zone of Ukraine by 2024 (Table 3).

Table 3: Spatial distribution of time-series parameters of LAI

Color	Range	Level	Area (km²)		Share (%)	
			2019-2021	2022-2024	2019-2021	2022-2024
	0-0.1	Very Low	52014	70116	40.83	55.04
	0.1-0.15	Low	60506	45855	47.5	36.0
	0.15-0.2	Medium	12283	8956	9.64	7.03
	0.2-0.25	High	1420	1324	1.11	1.04
	>0.25	Very High	1160	1133	0.91	0.89
Differences in the spatial distribution of time-series parameters of LAI						
		Decrease	91713		72	
		No Change	69		0.1	
		Increase	35608		27.9	

The share of LAI in the range of 0-0.1 increased to 14.2 % in the area 18102 km^2. Differences in the LAI spatial distribution for the two periods are shown in Fig. 9. The decrease in LAI share on an area of 91,713.25 km^2 was 72 %.

Fig. 9: Differences in the LAI spatial distribution during two periods

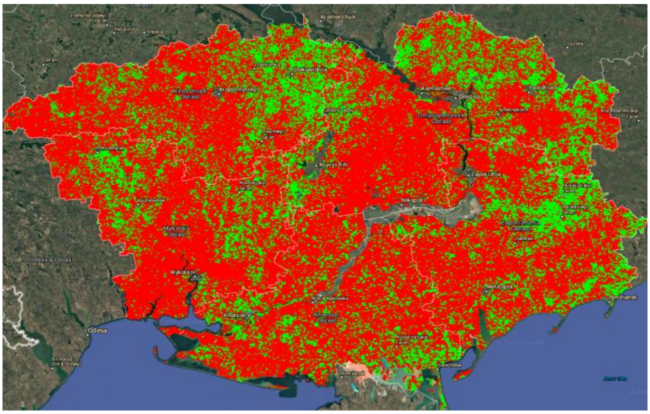

The maps of the spatial distribution of nitrogen dioxide across the steppe zone of Ukraine for the two compared periods are shown in Fig. 10. Analysis of the spatial distribution of nitrogen dioxide over the area of the northern part of the steppe of Ukraine shows that the main contribution to NO_2 pollution of the atmosphere is associated with the activity of industrial agglomerations located in such cities as Kryvyi Rih, Dnipro, Kamyanske, Nikopol, Zaporizhia and Chervonoarmiysk.

Fig. 10: The maps of the spatial distribution of NO_2 content in the atmosphere for two periods

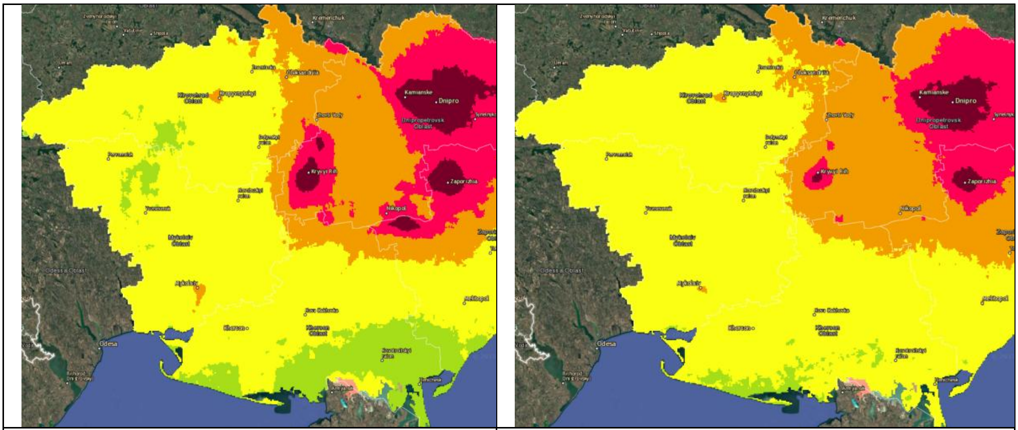

2019-2021	2022-2024

The decrease in the share of nitrogen dioxide from 0.00007 - 0.00008 mg/m^3 to 0-0.00007 mg/m^3 by the end of the period 2022-2024 was 7.36 % (Table 4).

Table 4: NO_2 spatial distribution, mg/m^3

Color	Range	Level	Area (km^2)		Share (%)	
			2019-2021	2022-2024	2019-2021	2022-2024
	0-0.00007	Very Low	11893	1853	8.7	1.36
	0.00007-0.000075	Low	71370	82516	52.3	60,5
	0.000075-0.00008	Medium	27695	32289	20.3	23.7
	0.00008-0.000085	High	19467	16959	14.3	12.4
	>0.000085	Very High	5937	2746	4.4	2.0
Differences in NO_2 spatial distribution						
		Decrease	61753		45	
		No Change	0		0	
		Increase	74609		55	

It is known that the main emissions of nitrogen dioxide into the atmosphere are associated with the blasting of ammonium in open-pit quarries for the extraction of iron ore (Kryvyi Rih and Shirokovsky districts of Dnipropetrovsk region), the operation of sintering plants of metallurgical plants and chemical industry enterprises. The reduction or complete absence of the area of NO_2 pollution halos in the Kryvbas iron ore and Nikopol manganese ore regions on the 2022-2024 map indicates a reduction or complete cessation of industrial activity in the southwest of the Dnipropetrovsk region, caused by the systematic bombing of these territories by Russian troops. The maps of the spatial distribution of sulfur dioxide across the steppe zone of Ukraine for the two periods being compared are shown in Fig. 11.

Fig. 11: The maps of the spatial distribution of SO_2 content in the atmosphere of the steppe zone of Ukraine for two periods

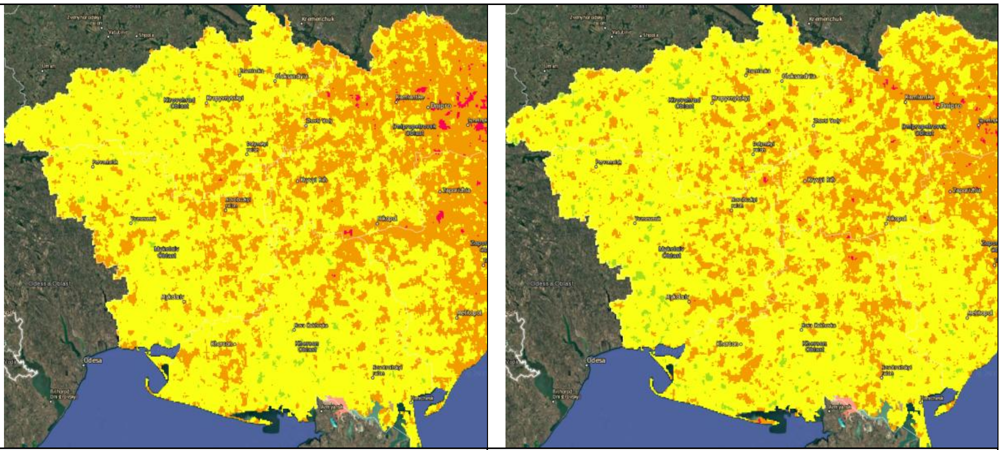

2019-2021	2022-2024

The main source of SO_2 atmospheric pollution is thermal power plants and mine dumps in the western Donbass. It is known that the removal of sulfide-containing minerals to the surface of mine dumps leads to the emission of SO_2 into the atmosphere during weathering (Plet *et al*., 2021). The decrease in the share of SO_2 with a concentration of >0.0002 mg/m^3 by the end of the period 2022-2024 was 9.0 % (Table 5).

Table 5: SO_2 spatial distribution, mg/m^3

Color	Range	Level	Area (km^2)		Share (%)	
			2019-2021	2022-2024	2019-2021	2022-2024
	0-0.0001	Very Low	1128	2089	0.8	1.5
	0.0001-0.00015	Low	22825	29936	16.7	22.0
	0.00015-0.0002	Medium	59066	63266	43.3	46.4
	0.0002-0.00025	High	40206	33440	29.5	24.5
	>0.00025	Very High	13137	7631	9.6.	5.6
Differences in SO_2 spatial distribution						
		Decrease	79823		58.5	
		No Change	0		0	
		Increase	56539		41.5	

The differences in the NO_2 and SO_2 spatial distribution in the steppe zone of Ukraine are shown in Fig. 12.

Fig. 12: The differences in the spatial distribution of time-series NO_2 and SO_2 in the steppe zone of Ukraine during two periods

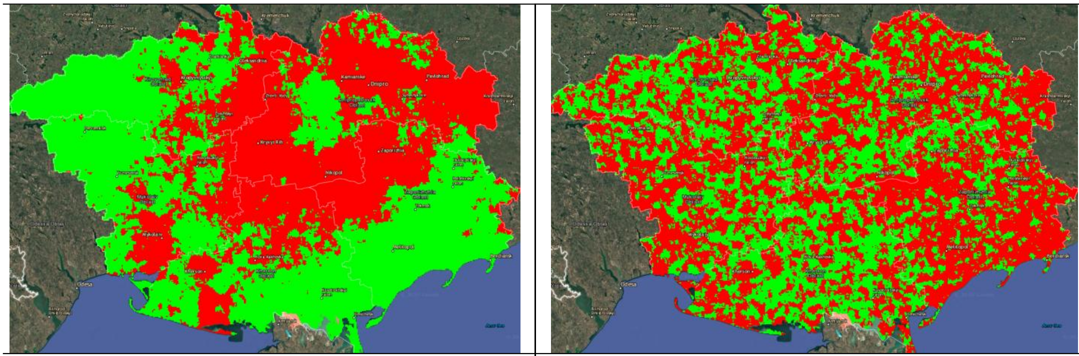

Changes in NO_2	Changes in SO_2

A visual assessment of the map of differences in the spatial distribution of NO_2 indicates that the main changes towards a decrease occurred in the central, industrially developed part of the northern steppe and the eastern and central parts of the steppe zone. In fact, a spatial dispersion of nitrogen dioxide from the central part of the steppe zone to adjacent territories occurred. A study of the SO_2 distribution map indicates a uniform distribution of local changes in the concentration of sulfur dioxide across the studied territory of the south-eastern part of Ukraine.

DISCUSSION

The advantages of used remote sensing indices

The monitoring and estimation of drought spatiotemporal dynamics on multiple time scales play a pivotal role in protecting the natural environment (Dejene *et al.*, 2023). Our current understanding of the use of SSM, LST and LAI indices is consistent with the results of a number of authors. Indeed, SSM and LST are closely interrelated (Pablos *et al.*, 2016). Integration of soil moisture indices (SMI) and land surface temperature (LST) makes it possible to conduct a comprehensive assessment of changes in soil moisture over time and space (Soni *et al.*, 2025). Data from three vegetation indices (VI) such as NDVI, NDWI, NDMI and LST were used to assess aridity over 30 years in Bangladesh (Das *et al.*, 2023). Our spatial assessment of changes in the soil surface moisture revealed the leading role of acute precipitation deficit in reducing plant evapotranspiration and, ultimately, in reducing SSM in the vast majority of the steppe zone of Ukraine. The creation of LST difference maps made it possible to identify areas of spatial changes in land surface temperature over the two compared periods, which started in the north-western, central, southern, and western steppe zones from April to September. The development of this approach seems similar to how it has been done in some studies (Wang *et al.*, 2021; Laz *et al.*, 2023; Passos *et al.*, 2024). The study of the temporal dynamics of the LAI and LST index revealed the significance of the corresponding seasonality of the vegetation cover (Ahmed *et al.*, 2024). The highest level of correlation between the leaf area index and the land surface temperature was in winter and autumn. The analysis of the LAI distribution maps for the two compared periods in our case confirmed that the severity of drought in the steppe zone of Ukraine has a horizontal zonality in the direction from south to north.

An original findings for development of knowledge in the regional level

Currently, four types of drought are distinguished, including meteorological, agricultural, hydrological and socio-economic droughts (Mishra & Singh, 2010; Zhang *et al*., 2022; Chen *et al*., 2024; Sutanto *et al*., 2024). In general, the droughts lead to degradation of land and vegetation cover, desertification and other consequences of natural disasters (Beloiu *et al*., 2022; Jalayer *et al*., 2022; Masroor *et al*., 2022; Bouwman *et al*., 2025).

It was found that in Ukraine, trends in meteorological drought characteristics are quite diverse on both a 3- and 12-month scale (Semenova & Serrano, 2024). The explosion of the Kakhovka dam in June 2023 in the south of the Dnipropetrovsk province can be an additional example initiated by military action drought (Pichura *et al*., 2025). It becomes clear that rising temperatures and precipitation variability are leading to an increase in the frequency of droughts in the south of Ukraine, where water availability is a limiting factor. Heat waves (above 33°C) increase evapotranspiration and pose a risk to plant growth in the steppe zone of the country. Potential weather extremes - frosts, heat waves, droughts, dust storms and heavy rainfalls - create variability in the spatial distribution of land surface temperature and soil moisture. For some time past, the dust storms of 8-17 h duration happened three to five times per year (Birmili *et al*., 2008). Meantime, atmospheric dust influences regional climate directly and indirectly by limiting incoming and outgoing solar radiation, precipitation formation, altering cloud properties atmospheric chemical processes. It is known that nitrogen and sulfur oxides are the main components of air pollution. Nitrogen oxides are key species in the troposphere, where they are linked to acid rain and ozone formation (Richter, 2009). Acidification lead to significant damage to ecosystems through exposure to air pollutants, nutrient imbalances in the soil, and foliar damage caused by ground-level ozone. In our case, the main halos of stable nitrogen dioxide are concentrated over the territories of industrial agglomerations in the Dnipropetrovsk, Zaporizhia and Donetsk provinces. Meanwhile, the main changes in the spatial distribution of nitrogen dioxide are noted in the eastern and southern parts of the steppe zone. Apparently, this is due to the processes of soil degradation caused by both the global warming process and the dominance of soil cultivation technologies, leading to the development of denitrification processes. It is also known that denitrification is an important component of the nitrogen cycle in soil, returning reactive nitrogen to the atmosphere (Schlüter *et al*., 2025). Denitrification is a four-step microbial-facilitated reduction process, whereby NO_3 is reduced to NO_2, NO, and N_2O (Hu *et al*., 2015). It was established that NO_x emissions were greater during the dry season at low (natural) soil nitrate content and comparable soil moisture (Cárdenas *et al*., 1993). It is also known that the main emissions of sulfur dioxide into the atmosphere are associated with the combustion of coal in thermal power plants and the operation of vehicles (Guttikunda & Jawahar, 2014; Wang *et al*., 2024). Studying the map of SO_2 distribution revealed a uniform distribution of local changes in the concentration of sulfur dioxide over the studied territory of south-eastern Ukraine.

International importance of original findings for development of knowledge in the regional drought occurence

It has been established that rising air temperatures coupled with low soil moisture lead to worsening drought (Semenova & Slizhe, 2020). In our case, analysis of key weather parameters and indices revealed that changes in air and land surface temperatures were insignificant, while precipitation decreased by more than half. The prevalence of very low soil moisture levels across much of Ukraine's steppe zone sets a precedent for the development of so-called general drought, which triggers a sharp drop in air humidity (Zhou *et al*., 2019). Particularly severe conditions are developing in the southern part of the

Ukrainian steppe, where over the past six years, evapotranspiration level have been 20 % lower than in the Kirovohrad and Dnipropetrovsk regions.

CONCLUSIONS

The results of this study allowed us to assess changes in surface temperature, soil moister and vegetation cover density in the northern and southern parts of the steppe zone of Ukraine. It was found that precipitation deficit and low surface moister are the dominant factors determining drought type. Visual assessment of the distribution of land surface temperature allows us to identify halos of spatial changes over a six-year period that occurred in the northwest, centre, south and western part of the steppe zone. Aridization led to a decrease in vegetation density over 72 % of the steppe zone in the direction from south to north.

The main changes in decreasing in the spatial distribution of NO_2 in the south-western part of Dnipropetrovsk region are connected with negative military impact of Russian troops on metallurgical plants activity.

CONFLICT OF INTEREST

The authors declare that they have no competing interests.

ACKNOWLEDGMENTS

This case study was supported by Ministry of Education and Science of Ukraine. It was also conducted under the Grant of the National Academy of Sciences of Ukraine to research laboratories/groups of young scientists in priority areas of science and technology (2025–2026) for the project "Development of a geoinformation toolbox for remote assessment of shelterbelts damaged by military actions"

REFERENCES

Ahmed, A.Y., Ali, A.M. & Ahmed, N. (2024). Temporal dynamics of leaf area index and land surface temperature correlation using Sentinel-2 and Landsat OLI data. *Environmental Systems Research*. 13, 43. https://doi.org/10.1186/s40068-024-00371-6

Alahacoon, N., & Edirisinghe, M. (2022). A comprehensive assessment of remote sensing and traditional based drought monitoring indices at global and regional scale. Geomatics, *Natural Hazards and Risk*. 13(1), 762–799. https://doi.org/10.1080/19475705.2022.2044394

Amiri, R., Weng, Q., Alimohammadi, A., & Alavipanah, S.K. (2009). Spatial-temporal dynamics of land surface temperature in relation to fractional vegetation cover and land use/cover in the Tabriz urban area, Iran. *Remote Sensing of Environment*. 113, 2606-2617.

Avdan, U. & Jovanovska, J. (2016). Algorithm for Automated Mapping of Land Surface Temperature Using LANDSAT 8 Satellite Data. *Journal of Sensors.* Article ID: 1480307. https://doi.org/10.1155/2016/1480307

Beloiu, M., Stahlmann R., & Beierkuhnlein, C. (2022). Drought impacts in forest canopy and deciduous tree saplings in Central European forests, *Forest Ecology and Management*. 509, 120075, https://doi.org/10.1016/j.foreco.2022.120075.

Birmili, W., Schepanski, K., Ansmann, A., Spindler, G., Tegen, I. et al. (2008). A case of extreme particulate matter concentrations over Central Europe caused by dust emitted over the southern Ukraine. *Atmospheric Chemistry and Physics*. 8 (4), 997-1016.

Bouwman, M., Akhmetzyanov, L., Mohren, F., den Ouden, J., Sass-Klaassen, U., & Copini, P. (2025). Tree growth responses to severe droughts for assessment of forest growth potential under future climate. *Forest Ecology and Management*, 578, 122423, https://doi.org/10.1016/j.foreco.2024.122423

Bulygin, S. (2006). Section 1.16. In book: *Soil erosion in Europe*. Editors, John Boardman, Jean Poesen. John Wiley & Sons Ltd, Chichester, England. 199-206.

Cárdenas, L., Rondón, A., Johansson, C., & Sanhueza E.(1993). Effects of soil moisture, temperature, and inorganic nitrogen on nitric oxide emissions from acidic tropical savannah soils. *Journal of Geophisical research atmospheres*. 98(D8),14783-14790. https://doi.org/10.1029/93JD01020

Carlson, T.N., J.K. Dodd, S.G. Benjamin & Cooper J.N. (1981). Satellite estimation of the surface energy balance, moisture availability and thermal inertia. *Journal of Applied Meteorology and Climatology*. 20, 67-87. https://doi.org/10.1175/1520-0450(1981) 020<0067:SEOTSE>2.0.CO;2

Chan, S., Bindlish, R., O'Neill, P., Jackson, T., Njoku, E., Dunbar, S., Chaubell, J., Piepmeier, J., Yueh, S., Entekhabi, D., Colliander, A., Chen, F., Cosh, M., Caldwell, T., Walker, J., Berg, A., McNairn, H., Thibeault, M., Martínez-Fernández, J., . . . Kerr, Y. (2017). Development and assessment of the SMAP enhanced passive soil moisture product. *Remote Sensing of Environment. 204*, 931–941. https://doi.org/10.1016/j.rse.2017.08.025

Chen, Y, Zhang, Y, Tian, J, Tang, Z, Wang, L, & Yang, X. (2024). Understanding the Propagation of Meteorological Drought to Groundwater Drought: A Case Study of the North China Plain. *Water*. 16(3):501. https://doi.org/10.3390/w16030501

Das, A.C., Shahriar, S.A., Chowdhury, M.A., Hossain, M.L., Mahmud, S., Tusar, M.K., Ahmed, R., & Salam, M.A. 2023.Assessment of remote sensing-based indices for drought monitoring in the north-western region of Bangladesh. *Heliyon*. 9(2):e13016. doi: 10.1016/j.heliyon.2023.e13016

Dejene, I.N, Moisa, M.B, Gemeda, D.O. 2023.Spatiotemporal monitoring of drought using satellite precipitation products: The case of Borena agro-pastoralists and pastoralists regions, South Ethiopia. *Heliyon*. 9(3):e13990. doi: 10.1016/j.heliyon.2023.e13990

Du, E, Dong, D, Zeng, X, Sun, Z, Jiang, X, & de Vries, W (2017). Direct effect of acid rain on leaf chlorophyll content of terrestrial plants in China. *Science of The Total Environment Journal*. 605:764–769. https://doi.org/10.1016/j.scitotenv.2017.06.044

Fileccia, T., Guadagni, M., Hovhera, V., & Bernoux M. (2014). *Ukraine: Soil fertility to strengthen climate resilience Preliminary assessment of the potential benefits of conservation agriculture*. Food and Agriculture Organization of the United Nations, 96p.

Gallo, K. P. & Owen, T.W. (1998). Assessment of Urban Heat Islands: A Multi-Sensor Perspective for the Dallas-Ft. Worth, USA Region. *Papers in Natural Resources*. 186. https://digitalcommons.unl.edu/natrespapers/186

Gong, C.; Xian, C.; & Ouyang, Z. (2022). Assessment of NO_2 Purification by Urban Forests Based on the i-Tree Eco Model: Case Study in Beijing, China. *Forests.13*, 369. https://doi.org/10.3390/f13030369

Goward, S. N. (1981). Thermal behavior of urban landscapes and the urban heat island. *Physical Geography.* 2(1), 19-33. https://doi.org/10.1080/02723646.1981.10642202

Goward, S.N., Xue, Y., & Czajkowski, K.P. (2002). Evaluating land surface moisture conditions from the remotely sensed temperature/vegetation index measurements: An exploration with the simplified simple biosphere model. *Remote Sensing in Environment.* 79, 225 - 242. https://doi.org/10.1016/S0034-4257(01)00275-9.

Guttikunda, S.K., & Jawahar, P. (2014). Atmospheric emissions and pollution from the coal-fired thermal power plants in India. *Atmospheric Environment*. 92, 449-460,https://doi.org/10.1016/j.atmosenv.2014.04.057

Hapich, H., & Onopriienko, D., (2024). Ecology and economics of irrigation in the south of Ukraine following destruction of the Kakhov reservoir. *International Journal of Environmental Studies.* 81(1), 301–314. https://doi.org/10.1080/00207233.2024.2314859

Hapich, H., Novitskyi, R., Onopriienko, D., Dent, D., & Roubik, H. (2024). Water security consequences of the Russia-Ukraine war and the post-war outlook. *Water Security, 21, 100167.* https://doi.org/10.1016/j.wasec.2024.100167

Hu, H. W., Chen, D., & He, J. Z. (2015). Microbial regulation of terrestrial nitrous oxide formation: understanding the biological pathways for prediction of emission rates. *FEMS Microbiology Reviews*. 39, 729–749. doi: 10.1093/femsre/fuv021

Huang, C., Chen, Q., Ying, S., Zhao, F., Shao, Y., Yu, W., Chen, J., Liu, F., Xin, X., & Li, J. (2009). An Analysis on the Coupling Relationship between Urban Vegetation and Land Surface Temperature in Hangzhou based on ASTER Imagery. *International Geoscience and Remote Sensing Symposium* (2009, Cape Town, South Africa), 3, 338-341. DOI:10.1109/IGARSS.2009.5417771

Jalayer, S., Sharifi, A., Abbasi-Moghadam, D., Tariq, A., & Qin, S.2022. Modeling and predicting land use land cover spatiotemporal changes: A case study in chalus watershed, Iran, *IEEE Journal of selected topics in applied earth observations and remote sensing*. 15, 5496–5513. doi: 10.1109/JSTARS.2022.3189528.

Jalayer, S., Sharifi, A., Abbasi-Moghadam, D., Tariq, A., & Qin, S.2023.Assessment of Spatiotemporal Characteristic of Droughts Using *In Situ* and Remote Sensing-Based Drought Indices. *IEEE Journal of selected topics in applied earth observations and remote sensing.*16,1483-1502 doi: 10.1109/JSTARS.2023.3237380

Karl, T.R., H.F. Diaz, & G. Kukla (1988). Urbanization: Its Detection and Effect in the United States Climate Record. *Journal Climate.* 1,1099-1123. https://doi.org/10.1175/1520-0442(1988)001<1099:UIDAEI>2.0.CO;2

Laz, O.U., Rahman, A., & Ouarda, T.B.M.J. (2023) Compound heatwave and drought hotspots and their trends in Southeast Australia. *Nat Hazards*. 119(1):357–386. https:// doi. org/ 10. 1007/s11069- 023- 06115-6

Liu, X., Fu, Z., Zhang, B., Zhai, L., Meng, M., Lin, J., & Zhang, J. (2018). Effects of sulfuric, nitric, and mixed acid rain on Chinese fir sapling growth in Southern China. *Ecotoxicology and Environmental Safety*. 160, 154–161. https://doi.org/10.1016/j.ecoenv.2018.04.071

Masroor, M., Sajjad, H., Rehman, S., Singh, R., Rahaman, M. H., Sahana, M., Ahmed, R., & Avtar, R. 2022. Analyzing the relationship between drought and soil erosion using vegetation health index and RUSLE models in Godavari middle sub - basin, India. *Geoscience Frontiers*, 13(2), 101312, https://doi.org/10.1016/j.gsf.2021.101312.

Mishra, A.K., & Singh, V.P. (2010). A review of drought concepts. *Journal of Hydrology*. 391(1–2), 202–216. https://doi.org/10.1016/j.jhydrol.2010.07.012.

Muñoz Sabater, J., (2019): *ERA5-Land monthly averaged data from 1981 to present [Data* *set]*. Copernicus Climate Change Service (C3S) Climate Data Store (CDS). https://doi.org/10.24381/cds.68d2bb30

Myneni, R., Knyazikhin, Y., & Park, T. (2015). *MCD15A3H MODIS/Terra+Aqua Leaf Area Index/FPAR 4-day L4 Global 500m SIN Grid V006* [Data set]. NASA EOSDIS *Land Processes DAAC*. http://doi.org/10.5067/MODIS/MCD15A3H.006

Orimoloye I.R. , Ololade O.O., Mazinyo S.P. , Kalumba A.M., Ekundayo O.Y. , Busayo E.T. , Akinsanola A.A., & Nel W. , (2019), Spatial assessment of drought severity in Cape Town area, South Africa, *Heliyon.* 5 (7), e02148.

Pablos, M., Martínez-Fernández, J., Piles, M, Sánchez, N., Vall-llossera, M., &Camps, A. 2016 .Multi-Temporal Evaluation of Soil Moisture and Land Surface Temperature Dynamics Using in Situ and Satellite Observations. *Remote Sensing*. 8(7):587. https://doi.org/10.3390/rs8070587

Passos, M.V., Kan, J.C., Destouni, G., Barquet K., & Kalantari Z. 2024. Identifying regional hotspots of heatwaves, droughts, floods, and their co-occurrences. *Stochastic Environmental Research and Risk Assessment* **38**, 3875–3893. https://doi.org/10.1007/s00477-024-02783-3

Pichura, V., Potravka, L., Stoiko, N., & Dudych, H. (2025). Scenarios for the functioning of the Kakhovka reservoir territory. *Journal of Landscape Ecology*. 18 (3), 118-154. DOI: 10.2478/jlecol-2025-0023

Payus, C.M., Jikilim, C., Sentian, J. (2020). Rainwater chemistry of acid precipitation occurrences due to long-range transboundary haze pollution and prolonged drought events during southwest monsoon season: climate change driven, *Heliyon*, 6(9),e04997, https://doi.org/10.1016/j.heliyon.2020.e04997

Plet, C., Siegel, C., Woltering,M., Noble, R., Pages, A., Thorne, R., Spinks, S., & Anand,R. (2021). Sulfur and CO_2 gases emitted during weathering of sulfides: Role of microbial activity and implications to exploration through cover, *Ore Geology Reviews.*134,104167. https://doi.org/10.1016/j.oregeorev.2021.104167.

Prakash, J., Agrawal, S.B. & Agrawal, M. (2023). Global Trends of Acidity in Rainfall and Its Impact on Plants and Soil. *Journal of Soil Science and Plant Nutrition*. 23, 398-419. https://doi.org/10.1007/s42729-022-01051-z

Running, S., Mu, Q., & Zhao, M. (2017). *MOD16A2 MODIS/Terra Net Evapotranspiration 8-Day L4 Global 500m SIN Grid V006 [Data set]*. NASA Land Processes Distributed Active Archive Center. https://doi.org/10.5067/MODIS/MOD16A2.006

Richter, A. (2009).Nitrogen oxides in the troposphere – What have we learned from satellite measurements? *European Physical Journal Conferences*. 1, 149-156. https://doi.org/10.1140/epjconf/e2009-00916-9

Sun, D. & Pinker, R.T. 2004.Case study of soil moisture effect on land surface temperature retrieval. *IEEE Journal of selected topics in applied earth observations and remote sensing.* 1, 127–130.

Schlüter, S., Lucas, M., Grosz, B., Ippisch, O., Zawallich, J., He, H., Dechow, R., Kraus, D., Blagodatsky, S., Senbayram, M., Kravchenko,·A., Vogel, H.J., Well R. (2025). The anaerobic soil volume as a controlling factor of denitrifcation: a review. *Biology and Fertility of Soils*. 61, 343–365. https://doi.org/10.1007/s00374-024-01819-8.

Sellers, P. J., & Schimel, D. S. (1993). Remote Sensing of the Land Biosphere and Biogeochemistry in the EOS Era: Science Priorities, Methods and Implementation - EOS Land Biosphere and Biogeochemical Panels. *Global Planet Change*. 7(4), 279-297.

http://dx.doi.org/10.1016/0921-8181(93)90002-6.

Semenova, I.& Serrano, V. (2024). Long-term variability and trends of meteorological droughts in Ukraine. *International journal of climatology*. 44(6),1849-1866. DOI: 10.1002/joc.8416.

Semenova, I.; Slizhe, M. (2020) Synoptic conditions of droughts and dry winds in the Black sea Steppe province under recent decades. *Front. Earth Sci. 8*, 69. doi:10.3389/feart.2020. 00069.

Smetana, S.M. & Crittenden, J.C.2014. Sustainable plants in urban parks: A life cycle analysis of traditional and alternative lawns in Georgia, USA. *Landscape and Urban Planning*.122, 140-151, https://doi.org/10.1016/j.landurbplan.2013.11.011.

Soni D., Yasmin S., Chandrakar A., Jangade A., & Garg A.K. 2025. Soil Moisture Index Estimation Using Land Surface Temperature Maps. *International journal of scientific research and technology.* 2(6), 643-646.

Sutanto, S.J., Syaehuddin, W.A. & de Graaf, I. (2024). Hydrological drought forecasts using precipitation data depend on catchment properties and human activities. Communications Earth & Environment. 5, 118. https://doi.org/10.1038/s43247-024-01295-w

Tian, Y., Dickinson, R. E., Zhou, L., Zeng, X., Dai, Y., Myneni, R. B., … & Shaikh, M. (2004). Comparison of seasonal and spatial variations of leaf area index and fraction of absorbed photosynthetically active radiation from moderate resolution imaging spectroradiometer (modis) and common land model. *Journal of Geophysical Research: Atmospheres*, 109(D1). https://doi.org/10.1029/2003jd003777

Veefkind, J., Aben, I., McMullan, K., Förster, H., De Vries, J., Otter, G., Claas, J., Eskes, H., De Haan, J., Kleipool, Q., Van Weele, M., Hasekamp, O., Hoogeveen, R., Landgraf, J., Snel, R., Tol, P., Ingmann, P., Voors, R., Kruizinga, B., . . . & Levelt, P. (2012). TROPOMI on the ESA Sentinel-5 Precursor: A GMES mission for global observations of the atmospheric composition for climate, air quality and ozone layer applications. *Remote Sensing of Environment. 120*, 70–83. https://doi.org/10.1016/j.rse.2011.09.027

Voogt, J. A. (2002). Urban Heat Island. In : Munn, T., ed., *Encyclopedia of Global Environmental Change*, 3, 660-666 (Chichester: Wiley).

Wan, Z., Hook, S., & Hulley, G. (2015). *MOD11A1 MODIS/Terra Land Surface Temperature/Emissivity Daily L3 Global 1km SIN Grid V006* [Data set]. NASA EOSDIS Land Processes Distributed Active Archive Center. https://doi.org/10.5067/MODIS/MOD11A1.006

Wang, W, Zhang, Y, Guo, B et al. (2021). Compound droughts and heatwaves over the Huai River Basin of China: from a perspective of the magnitude index. *Journal of hydrometeorology*. https:// doi. org/ 10. 1175/JHM-D- 20- 0305.1

Wang, F., Shaheen, A., Yousefi, R., Ge, Q., Wu, R., Lelieveld, J., Kaskaoutis, D. G., Lu, Z., Zhan, Y., & Zhou, Y. (2024). Long-Term Dynamics of Atmospheric Sulfur Dioxide in Urban and Rural Regions of China: Urbanization and Policy Impacts. *Remote Sensing*, *16*(2), 391. https://doi.org/10.3390/rs16020391

Weng, Q. **(**2009**).** Thermal Infrared Remote Sensing for Urban Climate and Environmental Studies: Methods, Applications, and Trends. *ISPRS Journal of Photogrammetry and Remote Sensing.* 64, 335–344. https://doi.org/10.1016/j.isprsjprs.2009.03.007

Weng, Q., Lu, D. & Schubring, J. (2004). Estimation of land surface temperature-vegetation abundance relationship for urban heat island studies. *Remote Sensing of Environment*. 89, 467-483. https://doi.org/10.1016/j.rse.2003.11.005

Wu, L., & Convertino M. (2025). Ecological corridor design for ecoclimatic regulation: Species as eco-engineers.*Ecological Indicators*. https://doi.org/10.1016/j.ecolind.2025.113149

Zhang, Y., Wu, Z., Singh, V.P., Jin, J., Zhou, Y., Xu, S., & Li, L. (2022). Agricultural Drought Assessment in a Typical Plain Region Based on Coupled Hydrology -Crop Growth Model and Remote Sensing Data. *Remote Sensing*. 14, 5994. https://doi.org/10.3390/rs14235994

Zhou, Y. . (2024). Long-Term Dynamics of Atmospheric Sulfur Dioxide in Urban and Rural Regions of China: Urbanization and Policy Impacts. *Remote Sensing.* 16, 391. https://doi.org/10.3390/rs16020391

Zhou, S., Williams, A.P., Berg, A.M., Cook, B.I., Zhang, Y., Hagemann, S., Lorenz, R., Seneviratne, S.I., Gentine, P. (2019). Land–atmosphere feedbacks exacerbate concurrent soil drought and atmospheric aridity. *Proc. Natl. Acad. Sci. USA 116*, 18848–18853, doi:10.1073/pnas.1904955116